Search for $1s2s\ ^3S_1-1s2p\ ^3P_2$ decay in U^{90+}

P. Beiersdorfer, S. R. Elliott,* A. Osterheld, Th. Stöhlker,† J. Autrey,‡ G. V. Brown,§ A. J. Smith,‡ and K. Widmann
Department of Physics and Space Technology, Lawrence Livermore National Laboratory, Livermore, California 94550
(Received 20 December 1995)

We present high-resolution crystal-spectrometer measurements that cover the wavelength range 3.0–3.2 Å containing the electric-dipole-allowed $2s_{1/2}$-$2p_{3/2}$ transitions in highly charged uranium ions. Strong features from $2s_{1/2}$-$2p_{3/2}$ transitions in lithiumlike, berylliumlike, and boronlike uranium were observed. In addition, a weak feature with intensity just above the level of background fluctuations was observed at the predicted location of the $1s2s\ ^3S_1-1s2p\ ^3P_2$ transition in heliumlike U^{90+}. The feature was observed in spectra where the intensity of the $2s_{1/2}$-$2p_{3/2}$ transition in lithiumlike uranium, and thus the ionization balance, was optimized; it appeared absent in spectra where the average ionization balance was lower. The measured energy of the feature is 4510.05 ± 0.24 eV, which agrees closely with the values predicted for the $1s2s\ ^3S_1-1s2p\ ^3P_2$ transition by recent theories. Detailed spectral modeling calculations indicate the possibility that a weak transition in berylliumlike U^{88+} is situated within 4 eV of the location of the heliumlike $^3S_1$-$^3P_2$ transition. This transition connects the level $1s\ ^2 2p_{1/2}2p_{3/2}\ ^3p_1$ with the $1s\ ^2 2s_{1/2}2p_{1/2}\ ^3P_0$ metastable ground level in berylliumlike uranium. The accuracy with which the energy of the berylliumlike transition can be predicted is insufficient to rule out a blend with the heliumlike $^3S_1$-$^3P_2$ transition. [S1050-2947(96)06906-5]

PACS number(s): 32.30.Rj, 12.20.Fv, 32.70.Fw, 31.30.Jv

I. INTRODUCTION

Heliumlike ions represent the simplest atomic system for developing and testing theoretical approaches for calculating the atomic structure of multielectron ions. In this case, the nonrelativistic Schrödinger equation can be solved with high accuracy so that many-body relativistic and quantum electrodynamical (QED) effects can be isolated and compared with measurement. In recent years, intense theoretical investigations have been undertaken to understand and calculate the contributions affecting the structure of heliumlike ions. Recent theoretical approaches to calculate the energy levels of the heliumlike ions and to enumerate the different contributions include the so-called unified method [1], the configuration-interaction (CI) approach [2,3], and the all-order method [4]. Comparisons among the results have evidenced significant differences that could be attributed to the order of expansion in $(Z\alpha)$ of the relativistic correlation and QED energies. These differences have increased the need for precise experimental data against which the various theoretical results can be gauged. Such a need is especially strong for data from heavy heliumlike ions with atomic number $Z>54$ for which almost no experimental values exist but for which relativistic and QED effects are most important.

Relativistic and QED effects are largest for the energy of the $1s^2$ ground state. In heliumlike U^{90+} QED effects represent 262.8 eV of the 129 566-eV ground-state energy [1]. QED effects are considerably smaller for the energy of a $2s$ electron (about 49 eV for U^{90+}). However, as a fraction of the transition energy measured in spectroscopic observations the QED contributions are maximized in $2s$-$2p$ transitions, and their energy can, in principle, be measured with high-resolution crystal spectrometers not yet available for measuring the $1s$-$2p$ transitions. Moreover, the natural width of the $2s$-$2p$ transitions is either about equal to or considerably smaller than that of the $1s$-$2p$ transitions. Measurements of $2s$-$2p$ transitions thus provide important tests of structure calculations complementary to measurements involving transitions to the ground state. Two $2s$-$2p$ transitions are possible in heliumlike ions: $1s2s\ ^3S_1-1s2p\ ^3P_0$ and $1s2s\ ^3S_1-1s2p\ ^3P_2$. These transitions have been measured in virtually all elements with $Z \leqslant 36$, as illustrated in a recent summary by Kukla *et al.* [5]. By contrast, we are aware of only one measurement for the energy of the $1s2s\ ^3S_1-1s2p\ ^3P_0$ transition in heliumlike ions with $Z>36$. This measurement was made by Munger and Gould in heliumlike U^{90+} and achieved an accuracy of 7.9 eV [6]. Similarly, only one measurement beyond krypton has been reported for the $1s2s\ ^3S_1-1s2p\ ^3P_2$ transition in heliumlike ions. This measurement was carried out by Martin *et al.* in Xe^{52+} with an accuracy of 1.74 eV [7]. In the present paper, we report experiments to identify and measure the latter transition in heliumlike U^{90+}.

The present experiments were carried out on the high-energy electron-beam ion trap (EBIT) facility at the Lawrence Livermore National Laboratory [8]. The facility was used earlier to measure the energy of $2s_{1/2}$-$2p_{3/2}$ transitions in lithiumlike through neonlike thorium and uranium [9–11]. A weak candidate feature, with an intensity 2.5 times larger than the standard deviation of the fluctuations of the background level and thus barely resolved, was identified in a set of measurements. Its energy was measured within a 0.24-eV uncertainty to be 4510.05 eV, in good agreement

*Present address: Nuclear Physics Laboratory, University of Washington, Seattle, WA 98195.
†Permanent address: Gesellschaft für Schwerionenforschung, Planckstrasse 1, D-64220 Darmstadt, Federal Republic of Germany.
‡Permanent address: Department of Physics, Morehouse College, Atlanta, GA 30314.
§Permanent address: Department of Physics, Auburn University, Auburn, AL 36839.

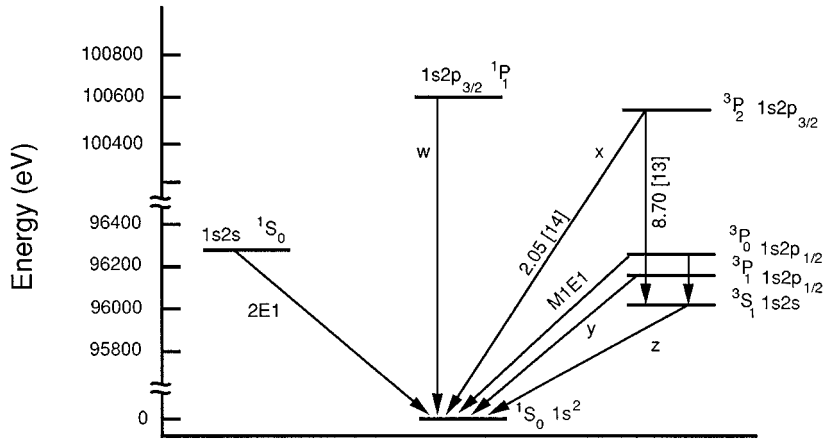

FIG. 1. Level diagram of heliumlike U^{90+}. Radiative rates for the decay of the $1s2p\ ^3P_2$ level from our collisional-radiative calculations are indicated (in units of s^{-1}). Square brackets denote powers of 10.

with the value predicted by various theoretical approaches for the energy of the $1s2s\ ^3S_1$–$1s2p\ ^3P_2$ transition. Measurements and calculations are presented to address the possibility that the feature is produced by a transition in a charge state lower than heliumlike uranium or by a contaminant indigenous to the trap. The possibility exists that the feature is produced by the transition $1s^22p_{1/2}2p_{3/2}\ ^3P_1 \rightarrow 1s^22s_{1/2}2p_{1/2}\ ^3P_0$ in berylliumlike U^{88+}. Because of the low electron density in EBIT ($\leqslant 5\times10^{12}$ cm^{-2}), this transition can be excited only from the berylliumlike $1s^22s_{1/2}2p_{1/2}\ ^3P_0$ metastable ground level. Its intensity, thus, is directly proportional to the population density of the berylliumlike $^3P_0$ metastable ground level. This transition has not yet been observed for any highly charged berylliumlike ion, and the accuracy with which its energy has been predicted is insufficient to rule out blending with the heliumlike $^3S_1$-$^3P_2$ transition. The results of our analysis of spectral features and excitation processes can be used in the design of future experiments for measuring transitions among excited states in highly charged heliumlike ions that extend to virtually all ions with $Z\leqslant 92$.

II. THEORETICAL CONSIDERATION

A diagram of the excited level structure in heliumlike uranium is shown in Fig. 1. There are six excited levels of the type $1s2l$. The levels $1s2p\ ^1P_1$, $1s2p\ ^3P_1$, and $1s2p\ ^3S_1$ decay directly to the $1s^2$ ground state by electric or magnetic dipole emission. A fourth, the level $1s2s\ ^1S_0$, decays by two-photon emission. Enabled by the hyperfine interaction, the $1s2p\ ^3P_0$ level decays directly to the ground state in ^{233}U or ^{235}U; in the absence of the hyperfine interaction, as is the case in ^{238}U, it decays by an intrashell transition to the $1s2s\ ^3S_1$ level or, at about half the rate, by two-photon emission to the $1s^2$ ground state.

The $1s2p\ ^3P_2$ level, of interest in the present study, decays either to the $1s^2$ ground state or by an intrashell transition to the $1s2s\ ^3S_1$ level. In low-Z ions, the $1s2p\ ^3P_2$ level decays exclusively to the $1s2s\ ^3S_1$ level [12]. However, in higher-Z ions the level decays increasingly via a magnetic quadrupole transition to the $1s^2$ ground state [12], as illustrated in Fig. 2. This trend reverses in very-high-Z ions, where relativistic effects again enhance the probability for dipole-allowed decay to the $1s2s\ ^3S_1$ level. Detection of this transition in high-Z ions is thus not precluded by an overwhelmingly large radiative branch to the $1s^2$ ground state. In heliumlike uranium, our radiative rates indicate a $^3S_1$-$^3P_2$ branching ratio of 30%.

In the relatively low electron densities in EBIT ($n_e\leqslant 5\times10^{12}$) electron-impact excitation proceeds only from the heliumlike $1s^2$ ground state. The cross sections for electron-impact excitation of a $1s$ electron to a $2p$ level are much smaller than those of a $2s$ electron to a $2p$ level. The abundance of heliumlike uranium ions at an electron energy of 140 keV is about equal to that of the lower charge states U^{89+} and U^{88+} and approaches 20% of the total, as predicted by Penetrante *et al.* [13]. We thus expect the intensity of the heliumlike $^3S_1$-$^3P_2$ transition to be much lower than comparable $2s_{1/2}$-$2p_{3/2}$ transitions in the low charge states of uranium. Using the relativistic distorted-wave code developed by Bar-Shalom, Klapisch, and Oreg [14] we calculated 3.9×10^{-25} cm^{-2} for the cross section of electron-impact excitation for the $1s2p\ ^3P_2$ level from ground for 140-keV electrons. This is about two orders of magnitude smaller than the cross section for the excitation of the $1s^22p_{3/2}\ ^2P_{3/2}$ level in lithiumlike uranium from the ground state, for which we calculated 1.2×10^{-22} cm^{-2}. The Breit interaction, missing in our calculations, is predicted to enhance the excitation

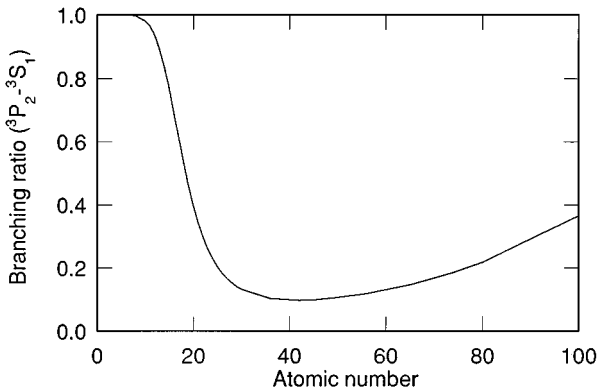

FIG. 2. Branching ratio for radiative decay of the $1s2p\ ^3P_2$ level to the $1s2s\ ^3S_1$ level in heliumlike ions. The ratio was computed from radiative rates reported in Ref. [12].

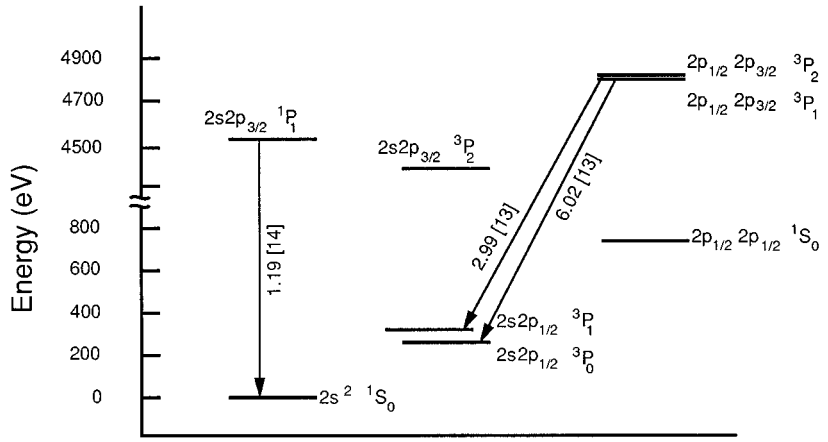

FIG. 3. Level diagram of berylliumlike U^{88+}. In the absence of hyperfine interaction with the nucleus, the level $1s^2 2s_{1/2} 2p_{1/2}\ ^3P_0$ is strictly forbidden to decay to the $1s^2 2s^2\ ^1S_0$ ground state. The level represents a ground level for the excitation of levels of the type $1s^2 2p_{1/2}^2$ and $1s^2 2p_{1/2} 2p_{3/2}$ that otherwise could not be populated from the $1s^2 2s^2\ ^1S_0$ level in a low-density electron beam. Radiative rates from our collisional-radiative calculations (in units of s^{-1}) are indicated. Square brackets denote powers of 10.

cross section of the heliumlike level by nearly a factor of 2 [15]. To account for the contributions from cascades, we constructed a collisional-radiative model for heliumlike U^{90+} which included all excitations to and all radiative cascades from levels of the type $1snl$ with $n \leqslant 5$. This model was based on the HULLAC set of computer codes employed in earlier analyses [11,16] and showed that radiative cascades from levels with $n \geqslant 3$ enhance the population of the $1s2p\ ^3P_2$ level by an additional factor of 2. The heliumlike $^3P_2$ level is also populated by radiative (and charge-exchange) recombination with hydrogenic U^{91+}. Using our radiative cascade model we find that about 8% of the electrons captured by hydrogenic uranium into excited levels feed the population of the heliumlike $^3P_2$ level. In equilibrium, the capture rate of U^{91+} is balanced by the ionization rate of U^{90+}, so that we estimate a 30% increase in the excitation cross section of the $^3P_2$ level. Our modeling, thus, shows that indirect excitation processes represent the largest contributors to the excitation of the $^3P_2$ level. Although the overall excitation cross section of the level, at about 2 b, remains almost two orders of magnitude lower than that of the lithiumlike $1s^2 2s_{1/2}$-$1s^2 2p_{3/2}$ transition, it is sufficient to form about 10^3 $^3P_2$ levels per second given about 5×10^4 U^{90+} ions in the trap.

The energy of the $1s2s\ ^3S_1 - 1s2p\ ^3P_2$ transition in heliumlike U^{90+} was predicted by Drake to be 4510.012 eV using the unified method [1]. This included 40.4 eV from QED calculated to order $(Z\alpha)^3$. Subsequently, Plante, Johnson, and Sapirstein performed an all-order calculation that resulted in a value of 4510.45 eV [4]. The same value for the QED contribution was used, and the difference was mainly a result of accounting for an additional term on the order of $(Z\alpha)^4$ in the relativistic electron correlation interaction, referred to by the authors as the ''structure contribution.'' Using a large-scale CI calculation, Chen, Cheng, and Johnson calculated 4510.64 eV [2]. Again, the same value of the QED contribution calculated by Drake was used.

Based on its predicted energy, the $^3S_1$-$^3P_2$ transition falls halfway between the strong $2s_{1/2}$-$2p_{3/2}$ electric-dipole transitions in berylliumlike U^{88+} and boronlike U^{87+}, which in an earlier measurement at the Livermore high-energy EBIT facility were measured at 4501.72 and 4521.39 eV, respectively [9]. The heliumlike transition thus does not blend with strong transitions from lower charge states. However, weak $2s_{1/2}$-$2p_{3/2}$ transitions from lower charge states of uranium could in principle compete in intensity and blend with the heliumlike transition in this spectral region. To examine this possibility we made extensive modeling calculations of the intensities of the $2s_{1/2}$-$2p_{3/2}$ transitions in lithiumlike through fluorinelike uranium. These modeling calculations are similar to those made earlier for the $2s_{1/2}$-$2p_{3/2}$ spectrum of thorium and uranium [11,16]. The calculations predict only one $2s_{1/2}$-$2p_{3/2}$ transition other than the heliumlike $^3S_1$-$^3P_2$ transition situated in this spectral range. This is the transition $1s^2 2p_{1/2} 2p_{3/2}\ ^3P_1 \rightarrow 1s^2 2s_{1/2} 2p_{1/2}\ ^3P_0$ in berylliumlike U^{88+}, which is excited from the $1s^2 2s_{1/2} 2p_{1/2}\ ^3P_0$ metastable level in ^{238}U. An overview of the level structure in berylliumlike uranium is given in Fig. 3. The intensity of the berylliumlike transition is predicted to be about 0.37% of that of the strong $1s^2 2s^2\ ^1S_0 - 1s^2 2s_{1/2} 2p_{3/2}\ ^1P_1$ transition, corresponding to an excitation cross section of 0.9 b, if no feeding of the $1s^2 2s2p\ ^3P_0$ level from radiative recombination from lithiumlike ions is included. With radiative-recombination feeding, our model predicts an intensity of 2.8%, or 6.7 b. The energy of this transition was predicted by our calculations to be 4513.7 eV. From our earlier study of the $2s_{1/2}$-$2p_{3/2}$ transitions in highly charged uranium [9] we know that the actual energy may differ by several eV from this value. In fact, our calculations give a value of 4505.6 eV for the strong berylliumlike $2s_{1/2}$-$2p_{3/2}$ transition. This value is 3.9 eV larger than measured. If we assume that the value predicted for the $1s^2 2p_{1/2} 2p_{3/2}\ ^3P_1 \rightarrow 1s^2 2s_{1/2} 2p_{1/2}\ ^3P_0$ transition is also 3.9 eV too high (which because of differing amounts of correlation effects may not be a good assumption), we get 4509.8 eV for its energy. This transition thus may blend and mask the heliumlike $1s2s\ ^3S_1 - 1s2p\ ^3P_2$ transition.

The $1s^2 2p_{1/2} 2p_{3/2}\ ^3P_1$ level decays back to the $1s^2 2s_{1/2} 2p_{1/2}\ ^3P_0$ level only 67% of the time. During the remainder it decays to the $1s^2 2s_{1/2} 2p_{1/2}\ ^3P_1$ level. As a result, excitation of the $^3P_0$ berylliumlike metastable ground level produces a second line with half of the intensity of the $1s^2 2p_{1/2} 2p_{3/2}\ ^3P_1 \rightarrow 1s^2 2s_{1/2} 2p_{1/2}\ ^3P_0$ transition. Our calculations predict the energy of the second line to be 4473.1 eV, or 4469.2 eV after a shift of 3.9 eV. The second peak thus falls into the region between the strong $2s_{1/2}$-$2p_{3/2}$ in

lithiumlike and berylliumlike uranium.

The hyperfine interaction depletes the population of the $1s^2 2s_{1/2} 2p_{1/2}\ ^1P_0$ level in uranium isotopes with odd nucleon number, and this transition does not exist in the ^{233}U or ^{235}U ions.

While our model calculations predicted no transitions from the lithiumlike through fluorinelike charge states other than the one transition in berylliumlike uranium that might blend with the heliumlike $1s2s\ ^3S_1$–$1s2p\ ^3P_2$ transition, it is possible that transitions from charge states lower than fluorinelike U^{81+} fall into this spectral region and mask the heliumlike transition. We have not made any calculations to check this possibility. Accurate predictions of the locations of weak transitions from such low charge states are presently impossible.

III. EXPERIMENTAL STUDIES

The region between the strong $2s_{1/2}$-$2p_{3/2}$ electric-dipole transitions in berylliumlike U^{88+} and boronlike U^{87+} was surveyed in an earlier measurement at the Livermore high-energy EBIT facility [9]. No feature that could be attributed to the $^3S_1$-$^3P_2$ transition was identified in these measurements. This was consistent with the smallness of the predicted excitation rates of the $1s2p\ ^3P_2$ level, the low counting statistics, and the relatively low ionization balance of the measurement. Similarly, no feature attributed to the $^3S_1$-$^3P_2$ transition was identified in measurements of the $2s_{1/2}$-$2p_{3/2}$ transitions in lithiumlike Th^{87+} and neonlike Th^{80+} [11]. In this case, the heliumlike $^3S_1$-$^3P_2$ transition was expected to blend with the strong $^1S_0$-$^1P_1$ transition in berylliumlike thorium and was impossible to resolve.

The present measurement was also performed on the high-energy EBIT. In our attempt to observe a statistically significant feature attributable to the heliumlike $^3S_1$-$^3P_2$ transition, we took the following measures.

First, we optimized the ionization balance to trap as much heliumlike uranium as possible. This was accomplished by reducing the amount of neutral gas injection (typically argon or neon) used for heavy-ion cooling and by increasing the current in the electron beam from 165 to about 190 mA. The latter minimizes charge-transfer reactions relative to electron-ion interactions. We also trapped the uranium ions in a shallow trap. This preferentially allows boiloff of lower charge states of uranium [17].

Second, we set the energy of the beam electrons to 140 keV, i.e., to an energy above the threshold for producing hydrogenic uranium. This value is considerably higher than that used in the earlier measurement of the $2s_{1/2}$-$2p_{3/2}$ transitions in lithiumlike through neonlike uranium [9].

Third, we increased the observation time to a total of 800 h. This is about eight times longer than the observation time in the earlier measurements.

Fourth, we increased the resolving power of the spectrometer by a factor of 2.5 in order to resolve potential blends. The increase was accomplished by employing a LiF(200) crystal with a 75-cm radius of curvature in the EBIT von Hámos–type spectrometer [18], supplanting the crystal with 30-cm radius of curvature used in the earlier measurement.

Two spectra covering the region of interest are shown in Fig. 4. The two strong berylliumlike and boronlike lines at

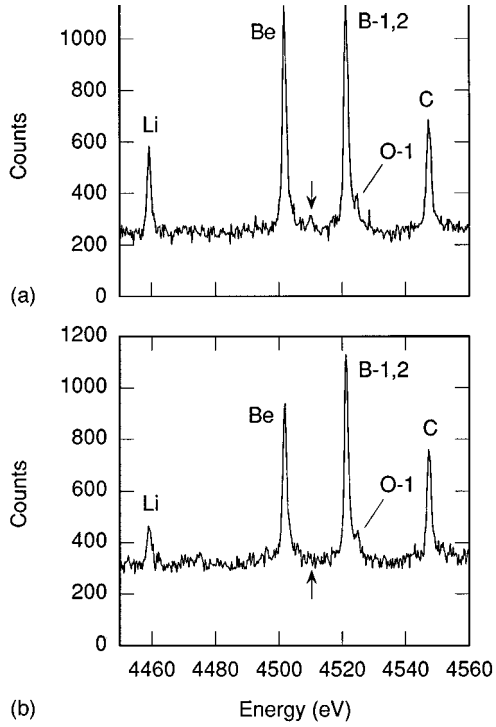

FIG. 4. Crystal-spectrometer spectra of the $2s_{1/2}$-$2p_{2/3}$ transitions in the energy region 4450–4560 eV: (a) ionization balance peaked near lithiumlike and berylliumlike uranium; (b) ionization balance peaked near boronlike uranium. Transitions in lithiumlike, berylliumlike, boronlike, carbonlike, and oxygenlike uranium are labeled by Li, Be, B, C, and O, respectively, using the notation of Ref. [9]. The location of the $1s2p\ ^3P_2$–$1s2s\ ^3S_1$ transition in heliumlike uranium is indicated by an arrow.

4501.72 and 4521.39 eV, respectively, are prominently seen. We used these two lines as reference standards to calibrate the spectrum. Also seen is the $2s_{1/2}$-$2p_{3/2}$ transition in lithiumlike uranium measured previously [9,10] to be at 4459.37 $\pm$0.21 eV. In the present spectra, we find 4459.55 eV for its energy, which is in excellent agreement with the previous measurement. The spectrum in Fig. 4(a) represents the sum of 400 h of observation time. Only those measurements were included in the sum for which the ratio of the lithiumlike to berylliumlike line intensities was larger than 0.32. The average ratio of the lithiumlike to berylliumlike line intensity in the summed spectrum is 0.36. The spectrum in Fig. 4(b) also represents the sum of 400 h of observation time. Only those measurements were included for which the ratio of the lithiumlike to berylliumlike line intensities was smaller than 0.28. The average ratio of the lithiumlike to berylliumlike line intensity in the summed spectra is 0.24. The ratio of the berylliumlike to boronlike line intensity is also reduced in this spectrum. The ionization balance in Fig. 4(b) is thus clearly lower than that in Fig. 4(a).

We monitored for the presence of possible high-Z contaminants using a high-purity germanium detector [11]. No such contaminants were identified. Nevertheless, to assure that the amount of possible contaminants did not vary, individual measurements included in Figs. 4(a) and 4(b) were recorded in an alternating fashion.

A comparison between the two spectra in Fig. 4 aids in identifying a potential feature from heliumlike uranium, as the fractional abundance of heliumlike uranium ions is sig-

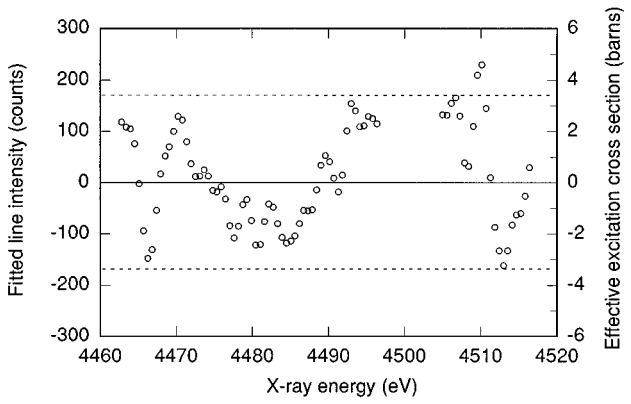

FIG. 5. Fitted intensity of a Gaussian-shaped trial function positioned at different spectral locations of the data of Fig. 4(a). The location of the strong berylliumlike line was excluded from the fit. The dashed lines indicate the value of two standard deviations in the fitted intensities. The intensity of the trial function peaks at the location of the candidate $^3S_1$-$^3P_2$ feature, reaching 236 counts or 2.5 standard deviations. The vertical scale on the right indicates the effective excitation cross section necessary to produce the corresponding number of counts in a given line. The scale was obtained by normalizing to the fitted intensities and corresponding excitation cross sections of the three strong lithiumlike, berylliumlike, and boronlike lines and assuming an equal abundance of the three ionization states.

nificantly reduced in Fig. 4(b) compared to that in Fig. 4(a). The intensity of a potential heliumlike transition should thus be significantly reduced relative to that of the strong berylliumlike line. In comparing the two figures, we identify a weak feature in Fig. 4(a) that represents a candidate for the $^3S_1$-$^3P_2$ heliumlike transition. As expected, it falls between the strong berylliumlike and boronlike transitions. It appears to be absent in the spectrum in Fig. 4(b).

To assess the validity of the feature in a quantitative way we used the following procedure. We constructed a Gaussian trial function with width equal to that determined for the strong berylliumlike line. Preselecting the position of the Gaussian and using a least-squares routine, we fitted the trial function together with a linear background term to the spectral region from 4460 to 4520 eV, i.e., to the region between the strong lithiumlike and boronlike lines. The location of the strong berylliumlike line was excluded in this procedure. By incrementing the position of the Gaussian trial function in steps of size one-third of its width we systematically probed the spectral region for locations of potential lines indicated by an increase in the fitted amplitude. The results of this scan applied to the data of Fig. 4(a) are given in Fig. 5, which shows the fitted intensities of the Gaussian trial function at the different spectral locations. Except at the location of the candidate $^3S_1$-$^3P_2$ feature, the intensity of the trial function ranged from -160 to $+165$ counts. By contrast, its intensity increased to 236 counts at the location of the candidate $^3S_1$-$^3P_2$ feature. This compares to a ''standard deviation'' of 85 counts in the overall variation of the fitted intensities. The intensity of the candidate feature thus rises about 2.5 ''standard deviations'' above the mean background level. Because the step size was less than the width of the trial function the fitted intensities are not statistically independent, and the use of ''standard deviation'' is not appropriate in a strict sense; nevertheless, it provides some measure of the significance of the feature in question.

TABLE I. Overview of measured transition energies.

Measurement	Energy (eV)
1	4510.38 ± 0.28 [a]
2	4509.86 ± 0.25 [a]
3	4509.82 ± 0.27 [a]
average	4510.05 ± 0.24 [b]

[a]Statistical uncertainty only.

[b]Statistical uncertainty combined with systematic uncertainty of the reference lines.

As another test of the nature of the candidate feature, we divided the measurements contributing to the spectrum in Fig. 4(a) into three data sets and checked to see whether the feature is present in each subset. Indeed, a weak feature was seen in each spectrum at essentially the same location. An overview of the energy inferred for the feature in each of the three subspectra is given in Table I. The average energy of the feature is 4510.05 eV. The combined uncertainties from purely statistical considerations as well as from the uncertainties of the energies of the berylliumlike and boronlike transitions used for calibration is 0.24 eV.

Because the hyperfine interaction with the nucleus quenches the $1s^2 2s 2p\ ^3P_0$ level in berylliumlike uranium and thus prevents excitation of the $1s^2 2p_{1/2} 2p_{3/2}\ ^3P_1 \rightarrow 1s^2 2s_{1/2} 2p_{1/2}\ ^3P_0$ transition, we have recorded a spectrum of the $2s_{1/2}$-$2p_{3/2}$ transition using ^{233}U and ^{235}U as target ions in the high-energy electron-beam ion trap. The hyperfine interaction may diminish the branching ratio for $^3S_1$-$^3P_2$ decay [19], but it cannot prevent it fully. ^{233}U was introduced into the trap using a thin, uranium-plated platinum wire, as described by Elliott and Marrs, instead of the usual injection by a metal vapor arc [20]. The resulting spectrum, obtained over a 100-h period, is shown in Fig. 6. A weak feature can be identified that is consistent with $^3S_1$-$^3P_2$ decay. The signal-to-noise ratio of the measurement and the associated fluctuation level in the background, however, prevent a definitive identification.

IV. DISCUSSION

Our spectral search, conducted over an 800-h observation period, yielded a weak feature with an intensity about 2.5 times larger than one standard deviation of the background level. The energy assigned to this feature is 4510.05 ± 0.24 eV. This is in excellent agreement with theoretical calculations for energy of the $^3S_1$-$^3P_2$ transition in heliumlike U^{90+}. Best agreement is found with the 4510.01-eV prediction of Drake [1]. Subsequent calculations by Chen, Cheng, and Johnson [2] and by Plante, Johnson, and Sapirstein [4] have shown that Drake's values should be augmented by a relativistic term of order $(Z\alpha)^4$. As mentioned above, these authors determined 4510.64 and 4510.45 eV for the $^3S_1$-$^3P_2$ transition energy. However, all three calculations include the same value for the QED contributions to the transition energy, which is only deemed accurate to order $(Z\alpha)^3$. The fact that our measured energy, provided it truly reflects that of the heliumlike $^3S_1$-$^3P_2$ transition, agrees best

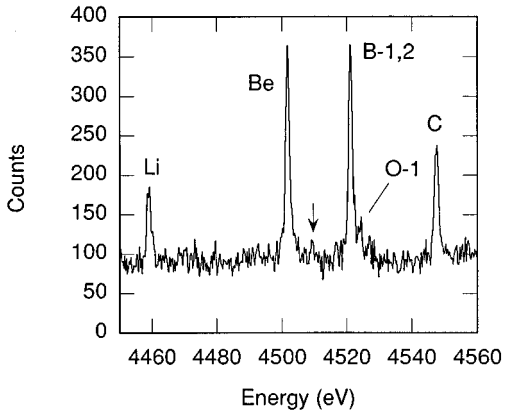

FIG. 6. Crystal-spectrometer spectrum of the $2s_{1/2}$-$2p_{2/3}$ transitions in the energy region 4450–4560 eV. The conditions are similar to those of Fig. 3(a), except that ^{233}U and ^{235}U were injected into the trap instead of ^{238}U. The location of the $1s2p\ ^3P_2$–$1s2s\ ^3S_1$ transition in heliumlike uranium is indicated by an arrow.

with Drake's value may thus be an indication that higher-order QED terms reduce the calculated transition energy.

The energy of the feature is also consistent with the energy of the transition $1s^22p_{1/2}2p_{3/2}\ ^3P_1 \rightarrow 1s^22s_{1/2}2p_{1/2}\ ^3P_0$ in berylliumlike U^{88+} for which the theoretical predictions are much less reliable than those for the heliumlike transition. Depending on the weight given to indirect excitation processes such as electron capture, ionization, and radiative cascades, the intensity of this line may be larger than that predicted for the heliumlike transition. In fact, the predicted intensity of the berylliumlike line agrees well with the intensity of the observed feature. By normalizing the fitted amplitude of the trial function plotted in Fig. 5 to the intensities and corresponding excitation cross sections of the three strong lithiumlike, berylliumlike, and boronlike lines, we can express the intensity of the observed feature in terms of an effective excitation cross section. According to Fig. 5, an effective cross section of up to 6×10^{-24} cm^{-2} is necessary to produce the feature. This is larger than the effective excitation cross section of the heliumlike $^3S_1$-$^3P_2$ transition, but is close to that of the berylliumlike $1s^22p_{1/2}2p_{3/2}\ ^3P_1 \rightarrow 1s^22s_{1/2}2p_{1/2}\ ^3P_0$ transition. The berylliumlike transition is accompanied by a second transition located near 4470 eV with half the intensity. While it is possible that this line forms the feature at 4470 eV in Fig. 5, we have not been able to discern a suitable candidate line directly from the spectral data.

The present analysis shows that lines with effective excitation cross sections near 1 b can be detected with our experimental techniques. Measurements with a yet lower detection limit and correspondingly better signal-to-noise ratio are needed to unambiguously identify the $^3S_1$-$^3P_2$ line. Future measurements might achieve a better signal-to-noise ratio by increasing the fraction of heliumlike ions or, better, by relying on the recombination of hydrogenlike ions to populate the $^3P_2$ level. In fact, our modeling calculations show that recombination is ten times more effective than electron-impact excitation in populating the $^3P_2$ level given equal abundances of hydrogenlike and heliumlike ions. Such conditions might be achieved in a high-energy electron-beam ion trap facility operating with a significantly higher beam energy than our present facility. Future measurements may also concentrate on using only ^{233}U or ^{235}U as target material in order to preclude blending with the berylliumlike $1s^22p_{1/2}2p_{3/2}\ ^3P_1 \rightarrow 1s^22s_{1/2}2p_{1/2}\ ^3P_0$ transition. Unambiguous identification of the heliumlike transition may also be achieved in a gas-jet-target experiment on a heavy-ion storage ring. Here, recombination is the primary method for exciting a particular transition, while charge-state selectivity eliminates blending with lines from different charge states, and coincidence techniques can be used to suppress background radiation [21].

ACKNOWLEDGMENTS

This work was supported in part by the Office of Basic Energy Science of the U.S. Department of Energy. Additional support was received from the Lawrence Livermore National Laboratory Research Collaborations Program for Historically Black Colleges and Universities. This work was performed under the auspices of the U.S. Department of Energy by Lawrence Livermore National Laboratory under Contract No. W-7405-ENG-48.

[1] G. W. F. Drake, Can. J. Phys. **66**, 586 (1988).
[2] M. H. Chen, K. T. Cheng, and W. R. Johnson, Phys. Rev. A **47**, 3692 (1993).
[3] K. T. Cheng, M. H. Chen, W. R. Johnson, and J. Sapirstein, Phys. Rev. A **50**, 247 (1994).
[4] D. R. Plante, W. R. Johnson, and J. Sapirstein, Phys. Rev. A **49**, 3519 (1994).
[5] K. W. Kukla, A. E. Livingston, J. Suleiman, H. G. Berry, R. W. Dunford, D. S. Gemmell, E. P. Kanter, S. Cheng, and L. J. Curtis, Phys. Rev. A **51**, 1905 (1995).
[6] C. T. Munger and H. Gould, Phys. Rev. Lett. **57**, 2927 (1986).
[7] S. Martin, J. P. Buchet, M. C. Buchet-Poulizac, A. Denis, J. Desesquelles, M. Druetta, J. P. Grandin, D. Hennecart, X. Husson, and D. Lecler, Europhys. Lett. **10**, 645 (1989).
[8] D. A. Knapp, R. E. Marrs, S. R. Elliott, E. W. Magee, and R. Zasadzinski, Nucl. Instrum. Methods Phys. Res. Sect. A **334**, 305 (1993).
[9] P. Beiersdorfer, D. Knapp, R. E. Marrs, S. R. Elliot, and M. H. Chen, Phys. Rev. Lett. **71**, 3939 (1993).
[10] P. Beiersdorfer, Nucl. Instrum. Methods Phys. Res. Sect. B **99**, 114 (1995).
[11] P. Beiersdorfer, A. Osterheld, S. R. Elliott, M. H. Chen, D. Knapp, and K. Reed, Phys. Rev. A **52**, 2693 (1995).
[12] C. D. Lin, W. R. Johnson, and A. Dalgarno, Phys. Rev. A **15**, 154 (1977).
[13] B. M. Penetrante, D. Schneider, R. E. Marrs, and J. N. Bardsley, Rev. Sci. Instrum. **63**, 2806 (1992).
[14] A. Bar-Shalom, M. Klapisch, and J. Oreg, Phys. Rev. A **38**, 1773 (1988).

[15] C. J. Fontes, D. H. Sampson, and H. L. Zhang, Phys. Rev. A **47**, 1009 (1993).

[16] V. Decaux, P. Beiersdorfer, and A. Osterheld, Nucl. Instrum. Methods Phys. Res. Sect. B **98**, 129 (1995).

[17] M. B. Schneider, M. A. Levine, C. L. Bennett, J. R. Henderson, D. A. Knapp, and R. E. Marrs, in *International Symposium on Electron Beam Ion Sources and their Applications–Upton, NY, 1988*, edited by A. Hershcovitch, AIP Conf. Proc. No. 188 (AIP, New York, 1989), p. 158.

[18] B. Beiersdorfer, R. E. Marrs, J. R. Henderson, D. A. Knapp, M. A. Levine, D. B. Platt, M. B. Schneider, D. A. Vogel, and K. L. Wong, Rev. Sci. Instrum. **61**, 2338 (1990).

[19] H. Gould, R. Marrus, and P. J. Mohr, Phys. Rev. Lett. **33**, 676 (1974).

[20] S. R. Elliott and R. E. Marrs, Nucl. Instrum. Methods Phys. Res. Sect. B **100**, 529 (1995).

[21] Th. Stöhlker, C. Kozhuharov, P. H. Mokler, A. Warczak, F. Bosch, H. Geissel, R. Moshammer, C. Scheidenberger, J. Eichler, A. Ichihara, T. Shirai, Z. Stachura, and P. Rymuza, Phys. Rev. A **51**, 2098 (1995).